Title

Is the Lecompte technique the last word on transposition of the great arteries repair for all patients? A magnetic resonance imaging study including a spiral technique two decades postoperatively.

Journal

Interactive cardiovascular and thoracic surgery, 22(6)

ISSN

1569-9293

Authors

Rickers, Carsten
Kheradvar, Arash
Sievers, Hans-Hinrich
et al.

Publication Date

2016-06-01

DOI

10.1093/icvts/ivw014

Peer reviewed

Interactive CardioVascular and Thoracic Surgery Advance Access published February 25, 2016

Interactive CardioVascular and Thoracic Surgery (2016) 1–9
doi:10.1093/icvts/ivw014

Cite this article as: Rickers C, Kheradvar A, Sievers H-H, Falahatpisheh A, Wegner P, Gabbert D *et al*. Is the Lecompte technique the last word on transposition of the great arteries repair for all patients? A magnetic resonance imaging study including a spiral technique two decades postoperatively. Interact CardioVasc Thorac Surg 2016; doi:10.1093/icvts/ivw014.

Is the Lecompte technique the last word on transposition of the great arteries repair for all patients? A magnetic resonance imaging study including a spiral technique two decades postoperatively

Carsten Rickers[a,*], Arash Kheradvar[b], Hans-Hinrich Sievers[c], Ahmad Falahatpisheh[b], Philip Wegner[a], Dominik Gabbert[a], Michael Jerosch-Herold[d], Chris Hart[a], Inga Voges[a], Léon M. Putman[c], Ines Kristo[a], Gunther Fischer[a], Jens Scheewe[a] and Hans-Heiner Kramer[a]

[a] Department of Congenital Heart Disease and Pediatric Cardiology, University Hospital of Schleswig-Holstein, Campus Kiel, Kiel, Germany
[b] University of California Irvine, Edwards Lifesciences Center of Advanced Cardiovascular Technology, Irvine, CA, USA
[c] Department of Cardiac and Thoracic Vascular Surgery, University Hospital of Schleswig-Holstein, Campus Luebeck, Luebeck, Germany
[d] Department of Radiology, Brigham & Women's Hospital & Harvard Medical School, Boston, MA, USA

* Corresponding author. Department of Congenital Heart Disease and Pediatric Cardiology, University Hospital of Schleswig-Holstein, Campus Kiel, Arnold-Heller-Str. 3, 24105 Kiel, Germany. Tel: +49-431-5971728; fax: +49-431-5971828; e-mail: carsten.rickers@uksh.de (C. Rickers).

Received 29 September 2015; received in revised form 1 December 2015; accepted 11 December 2015

Abstract

OBJECTIVES: To compare the Lecompte technique and the spiral anastomosis (complete anatomic correction) two decades after arterial switch operation (ASO).

METHODS: Nine patients after primary ASO with Lecompte and 6 selected patients after spiral anastomosis were evaluated 20.8 ± 2.1 years after ASO versus matched controls. Blood flow dynamics and flow profiles (e.g. vorticity, helicity) in the great arteries were quantified from time-resolved 3D magnetic resonance imaging (MRI) phase contrast flow measurements (4D flow MR) in addition to a comprehensive anatomical and functional cardiovascular MRI analysis.

RESULTS: Compared with spiral reconstruction, patients with Lecompte showed more vortex formation, supranatural helical blood flow (relative helicity in aorta: 0.036 vs 0.089; $P < 0.01$), a reduced indexed cross-sectional area of the left pulmonary artery (155 vs 85 mm²/m²; $P < 0.001$) and more semilunar valve dysfunctions ($n = 5$ vs 1). There was no difference in elastic aortic wall properties, ventricular function, myocardial perfusion and myocardial fibrosis between the two groups. Cross-sectional area of the aortic sinus was larger in patients than in controls (669 vs 411 mm²/m²; $P < 0.01$). In the spiral group, the pulmonary root was rotated after ASO more towards the normal left position ($P < 0.01$).

CONCLUSIONS: In this study, selected patients with spiral anastomoses showed, two decades after ASO, better physiologically adapted blood flow dynamics, and attained a closer to normal anatomical position of their great arteries, as well as less valve dysfunction. Considering the limitations related to the small number of patients and the novel MRI imaging techniques, these data may provoke reconsidering the optimal surgical approaches to transposition of the great arteries repair.

Keywords: Transposition of great vessels • Magnetic resonance imaging • Lecompte technique • Physiological spiral anastomosis

INTRODUCTION

Dextro-transposition of the great arteries (D-TGA) is the second most frequent cyanotic congenital cardiovascular malformation leading to early death in most cases, if left untreated [1]. In 1975, Jatene *et al.* [2] performed the first successful anatomical correction of complex TGA retransposed in the physiological spiral arrangement. Lecompte *et al*. [3] introduced a method in the early 1980s, which is characterized by placing the pulmonary artery bifurcation in front of the ascending aorta representing the current routine surgical technique for arterial switch operation (ASO) [4]. Since then, short-term surgical results have been reported to be excellent with low mortality [5]. Long-term follow-up data revealed also excellent clinical results in the majority of patients but showed some rare drawbacks, including pulmonary stenosis [6], dilatation of ascending aorta [7], diastolic dysfunction [8], aortic stiffening [9] and even progressive aortic regurgitation [10], the latter potentially due to the steeply angled aortic arch

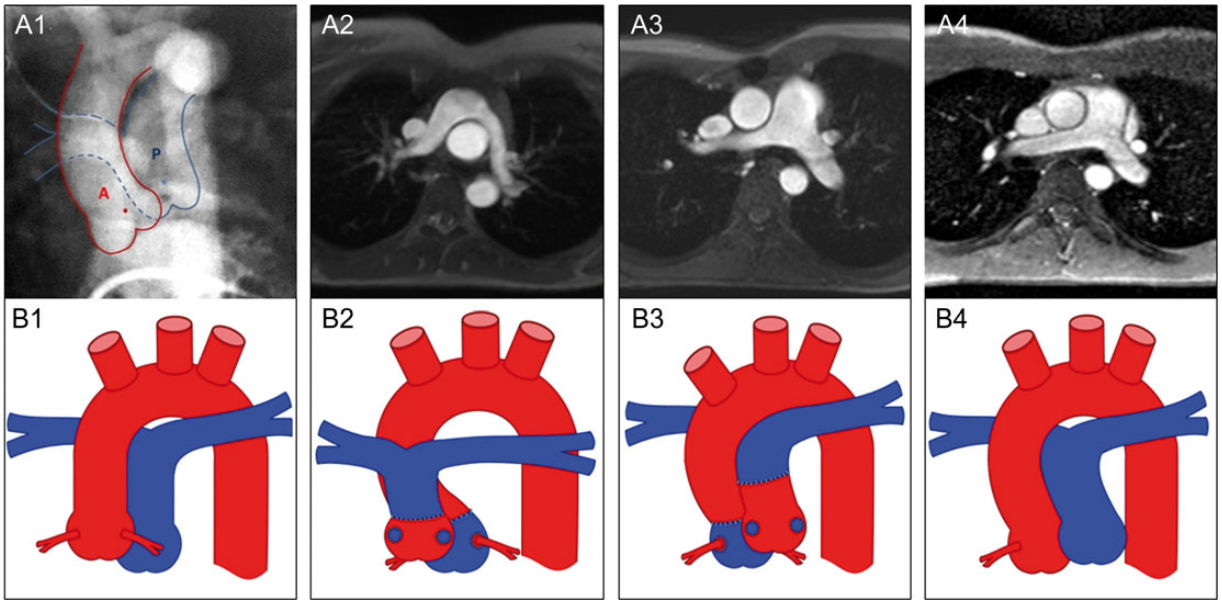

Figure 1: Morphology of the pulmonary arteries. Preoperative cinecardioangiogram (anterior–posterior projection) of a patient with simple D-TGA showing the centre points of the aortic (red dot) and pulmonary root (blue dot) (1). Anatomy of the great arteries 20 years after primary ASO, comparing the Lecompte technique (2) and the spiral anastomosis (3) and normal configured pulmonary arteries in a healthy control (4) illustrated by MRI (axial views) (upper row) and as a schematic drawing (lower row, red colour: aorta, blue colour: pulmonary artery). The steep aortic arch is illustrated by the smaller distance between the ascending and descending aorta in the Lecompte technique and the riding of the pulmonary bifurcation on the aorta. The post rotational more leftward position of the pulmonary root is shown in a patient with a spiral anastomosis (3a) and the corresponding schematic drawing (3b). A: aorta; P: pulmonary artery; D-TGA: dextro-transposition of the great arteries; ASO: arterial switch operation; MRI: magnetic resonance imaging.

after ASO [11]. These adverse long-term outcomes have prompted the evaluation of alternative surgical techniques [11, 12]. In the present study, we evaluated a cohort of consecutively corrected TGA patients, who received either a primary arterial switch with the Lecompte technique or physiological spiral anastomoses of the great arteries 20 years ago (Fig. 1).

Cardiovascular magnetic resonance imaging (MRI) was used to comprehensively evaluate cardiovascular anatomy and function, including novel 3D time-resolved phase contrast MRI techniques (4D-flow) to assess blood flow dynamics in patients and controls.

MATERIALS AND METHODS

Patients

Nine patients who underwent the Lecompte technique and 6 patients who underwent restoration of the spiral anatomic arrangement of the great vessels were studied at a mean of 20.8 ± 2.1 years after primary ASO in simple TGA (Supplementary Tables S1 and S2). All patients were operated by one of the authors (Hans-Hinrich Sievers) at the University of Kiel. This small series was stopped because the surgeon moved for a chief position to the University of Lübeck, where paediatric cardiac surgery was not practised. Moreover, five healthy volunteers of similar age were selected as control subjects (Supplementary Table S2). The study protocol was approved by the local research ethics committee and informed consent was obtained from all patients and volunteers.

Description of surgical techniques

The Lecompte technique was performed as described [3]. Spiral anastomoses were performed in selected patients preferably with less pronounced rotation of the aortic root to the right of the pulmonary root as assessed by the surgeon although there was no significant difference in preoperative pulmonary to aortic artery angle (Table 1). Postoperative calculations show that the spiral anastomoses were limited to a morphological situation where the angle between the pulmonary and aortic root does not exceed 45° rightward rotation of the aortic root to the anterior–posterior position (mean −32° ± 15°, Table 1). This rotation in the Lecompte group was slightly more (8°, mean −40° ± 25°, Table 1). Together, the spatial state of the great arteries in patients with a spiral anastomosis was between the anterior–posterior and the side-by-side configuration. In order to prevent tension and torsion of the neopulmonary artery and avoid potential compression of the left coronary artery, additional length for the neopulmonary artery was gained by transecting the aorta more distally than in the Lecompte technique. Furthermore, liberal mobilization of the ascending aorta and the arch as well as the pulmonary artery was performed. The pulmonary artery was completely released from the aorta and mobilized into the hila on the left and right side after transection in the middle of the pulmonary trunk. The coronary arteries were transposed, and then the aorta was anastomosed to the pulmonary root with 6/0 continuous polypropylene. The left coronary artery was tried to be placed in the pulmonary root as leftwards and as proximal as possible to prevent interference with the aortic root after being anastomosed to the distal pulmonary artery. In all patients, the conal branch of the left anterior descending coronary artery (LAD) was not sacrificed in those days; however, this surgical step could facilitate the spiral technique and make it safer against compression of the LAD. Thereafter, the distal pulmonary trunk was anastomosed to the proximal aorta using 6/0 polypropylene continuously. In one case with a 45° shift of the aortic root rightward and in front of the pulmonary artery, a 1 cm wide strip of autologous pericardium was used to enable the spiral anastomosis between the distal pulmonary artery and the

Table 1: Morphology

	Lecompte ($n = 9$)	Spiral ($n = 6$)	Control ($n = 5$)	p1	p2	p3
Max. aortic area (cm^2)						
Aortic root	13.7 ± 5.4	12.4 ± 0.2	7.7 ± 1.8	n.s.	0.018	0.035
Ascending aorta	7.3 ± 1.5	6.3 ± 1.0	6.8 ± 1.6	0.018	n.s.	n.s.
Aortic arch	5.3 ± 1.2	3.9 ± 0.7	4.7 ± 1.2	n.s.	n.s.	n.s.
Descending aorta at isthmus	3.6 ± 0.7	3.3 ± 0.7	3.1 ± 0.6	n.s.	n.s.	n.s.
Descending aorta at diaphragm	3.4 ± 0.8	2.7 ± 0.6	2.9 ± 0.9	n.s.	n.s.	n.s.
Max. pulmonary area (cm^2)						
Main PA	4.6 ± 1.0	5.6 ± 2.0	5.9 ± 1.4	n.s.	n.s.	n.s.
Right PA	2.0 ± 0.7	2.0 ± 1.1	2.5 ± 0.5	n.s.	n.s.	n.s.
Left PA	1.6 ± 0.4	2.8 ± 0.6	2.7 ± 0.5	0.001	n.s.	n.s
Aortic arch angle (°)	50 ± 4	61 ± 6	–	0.012	–	–
Angle PA to Ao, preoperation (°)	−40 ± 25	−32 ± 15	–	n.s.	–	–
Angle PA to Ao, postoperation (°)	−14 ± 20	38 ± 14	58 ± 5	0.006	0.001	0.001

Data presented as mean ± standard deviation. *P*-values refer to a comparison of groups: Lecompte and Spiral (p1), controls and TGA (p2) and all groups (p3). PA: pulmonary artery; Ao: aorta.

aortic root without tension and torsion. The incidence of ventricular septal defect was zero and no trap-door techniques were used for coronary artery anastomosis. We now believe that this latter surgical manoeuvre could facilitate the spiral technique to prevent potential LAD tension.

Determination of the pre- and postoperative angle between the aortic and pulmonary root

From a cinecardioangiogram in anterior–posterior projection, the centres of the aortic and pulmonary roots, and the diameters at this level were determined. The distance between the centre points and the diameters allowed for calculation of the angle of the roots of the great arteries (Fig. 1A, Supplementary Fig. S1). The postoperative angle was determined from axial cine MRI. As illustrated in Supplementary Fig. S2, the angle was measured from the connecting line of the centres of the aortic and pulmonary roots and the sagittal line through the aortic root.

Comprehensive magnetic resonance imaging examination

MRI studies were performed on a 3.0 Tesla scanner (Achieva 3.0T, X-series, Philips Medical Systems, Netherlands) and a phased-array coil for cardiac imaging. Electrocardiography (ECG)-triggered cine series were obtained using a balanced steady-state-free precession cine sequence with the voxel size of 2.5 × 2.5 × 7 mm; repetition time/echo time of 4.0/2.5 ms and flip angle of 10° and temporal resolution of 45 ms axial-, short-axis- and four-chamber-views for left and right ventricular function analysis were acquired by cine MRI. The images were analysed with dedicated software (Extended MR WorkSpace, version 2.6.3.2 HF3 2010, Philips Medical Systems).

Myocardial perfusion images were acquired during the first pass of intravenous-injected low dosage contrast bolus (0.03 mmol/kg of Magnevist) with an ECG-gated, single-shot, saturation-recovery-prepared, gradient echo sequence with the following parameters: TE/TR/flip angle: 1/2.3 ms/18°, 192 × 160 acquisition matrix, parallel imaging with sensitivity encoding x2 acceleration, slice: 10 mm, 2 slices at basal and mid-level per R-R interval in short-axis orientation, 60 dynamics. For assessment of the hyperaemic response, adenosine was infused with a step-wise dose incrementation from 50 to 100 µg/kg/min, and 140 µg/kg/min, lasting 9 min (3 min per stage) [13]. Myocardial perfusion was quantified in ml/min/g, by deconvolution of the signal-enhancement versus time curves for myocardial segments with the arterial contrast enhancement curves, measured in the centre of the left ventricular cavity. Briefly, and as previously described, the perfusion images were segmented along the endo- and epi-cardial borders, and the myocardium was divided into six segments for the basal and mid-level slices.

For characterization of myocardial scar tissue, late gadolinium enhancement (LGE) imaging 10–15 min after contrast injection (Magnevist, Bayer Pharma AG, Berlin, Germany; 0.1 mmol/kg) was measured using an ECG-triggered 3D inversion recovery sequence in the same short-axis planes that were used for cine imaging (field of view 300 × 178 × 80 mm [3]; voxel size 1.4 × 1.4 × 10 mm; repetition time/echo time 3.7/1.83 ms; flip angle 12°). LGE was quantified by using the mean signal and standard deviation (SD) in a region of interest in normal-appearing myocardium as reference, and setting a threshold of four SDs above the mean for normal myocardium as threshold for LGE.

Aortic dimensions and the aortic lumen area (for assessment of aortic distensibility) were measured by gradient echo cine imaging with retrospective ECG gating, using a stack of parallel, contiguous, 5 mm thick slices perpendicular to the aortic axis that were acquired at each measurement point (Supplementary Fig. S3) to determine the maximum and minimum aortic diameter as described previously by our group [9, 14].

Flow measurements

Time-resolved 3D phase contrast cine imaging, referred to as '4D-Flow MR', was performed with retrospective ECG and respiratory gating to measure cardiovascular blood flow in an axial slab of 30 × 30 × 15 cm^3 over 25 cardiac phases. The isotopic voxel dimension was 2.5 mm and the maximum encoding velocity was set at 300 cm/s. Evaluation of flow and visualization of the streamlines was performed with the flow analysis software GTFlow 2.1.4 (GyroTools GmbH, Winterthur, Switzerland) and 4DFloWorks, an in-house software for reading and processing 4D flow MR datasets developed at the University of California, Irvine, USA.

Fluid dynamics analysis

The blood flow dynamics was examined using the novel software 4DFloWorks for computation of the helicity and relative helicity defined below. The basic quantity describing the rotation of a velocity vector field ($\vec{u}$) is the vorticity $\vec{\omega}$:

$$\vec{\omega} = \text{rot}\,\vec{u} = \vec{\nabla} \times \vec{u} \quad (1)$$

where $\vec{\nabla}\times$ is the curl operator, a vector function that here describes the infinitesimal rotation of the 3D blood flow velocity vector field. The vorticity vector points into the direction of flow-helix axis when the helix is right-handed, and in the opposite direction if left-handed. Helicity (H) describes the tendency of the fluid flow through a cross-sectional area 'A' to follow a helical flow pattern associated with a net forward flow according to the following equation:

$$H = \int_A \vec{u} \cdot \vec{\omega}\, dV = \int_A \vec{u} \cdot (\vec{\nabla} \times \vec{u})\, dV \quad (2)$$

Helicity is a pseudoscalar quantity, and its sign reflects the direction of rotation; being positive for a right-handed helix, and negative for left-handed helical flow patterns. The relative helicity is quantified as a dimensionless quantity, namely by the cosine of the angle α between the velocity vector $\vec{u}$ and the vorticity vector $\vec{\omega}$:

$$H_{\text{rel}} = \frac{1}{V}\int_V \frac{\vec{u} \cdot \vec{\omega}}{|\vec{u}| \cdot |\vec{\omega}|} dV = \frac{1}{V}\int_V \cos\alpha dV \quad (3)$$

High magnitude values of relative helicity are obtained when velocity and vorticity are aligned or antialigned ($\alpha = 0°$ or $\alpha = 180°$). For the analysis of vessel area and through-plane velocity in the large vessels, eight positions were defined as follows (Supplementary Fig. S3):

(i) aortic root (sinus Valsalva): about 1 cm above the aortic valve;
(ii) ascending aorta in the middle of the ascending aorta;
(iii) aortic arch: highest peak of the arch, perpendicular to the vessel;
(iv) aortic isthmus: at the height of the pulmonary bifurcation;
(v) descending aorta: at the level of the diaphragm;
(vi) main pulmonary artery: in between pulmonary valve and bifurcation
(vii) (1.5 cm above the valve plane);
(viii) right pulmonary artery: usually 1–1.5 cm distal to the pulmonary bifurcation;
(ix) left pulmonary artery: ~1–1.5 cm distal to the pulmonary bifurcation.

Peak through-plane velocity (v_{max}) was determined for orthogonal cross-sectional planes at the predefined positions from 4D flow MR data. This task was accomplished by multiplanar reconstruction using GTFlow. In the orthogonal cross-sectional planes, vessel area and v_{max} were determined within manually drawn vessel contours.

The acquired 4D flow data were first converted to physical velocity fields using 4DFloWorks. The identification of the vessels was performed by a time-resolved phase contrast angiography with following relation:

$$\text{vessel} = \text{PV}_{\text{AM}}\sqrt{u^2 + v^2 + w^2} \quad (4)$$

where PV_{AM} is the pixel value of the anatomical magnitude image and (u, v, w) are the components of the velocity vector in the 4D flow MR image set. The physical velocity fields, as well as the computed vessel wall quantity, were exported from 4DFloWorks to Ensight (Computational Engineering International, Inc., Apex, NC, USA). The isosurface of the vessel at peak systole was chosen as the geometry of the vessel and stored in the stereolithography format using Ensight. In order to obtain the volume segments whose boundaries were determined according to our defined eight positions (Supplementary Fig. S2), we used the open source software Meshlab (distributed through meshlab.sourceforge.net). Using Meshlab, we cropped the vessels and obtained six vessel segments. These volume segments were imported back to 4DFloWorks as stereolithography format for computation of helicity. 4DFloWorks identified the points within the so-defined vessel segments. Having these points identified for each vessel segments, we computed the helicity according to equation (2). The global relative helicity was obtained by averaging relative helicity over segments corresponding to either aorta or pulmonary arteries.

The absolute values of relative helicity in the segments were averaged in order to obtain the relative helicity *magnitude*. The reconstruction of pathlines with GTFlow was used for a visual evaluation of vortex and helix formation. The blood flow dynamics in each case was checked for the presence of vortex formation. Helical scale was graded separately using the following grading scale: 0, small helix formation (flow rotation <180°); 1, moderate, supraphysiologic-helix (flow helix <360°); 2, pronounced supraphysiologic-helix (flow rotation >360°).

Statistical analysis

All statistical analyses were performed using commercially available software (SPSS 21.0; SPSS, Inc., Chicago, USA). The Mann–Whitney *U*-test for independent samples was used to compare the Lecompte group with the spiral group (p1) and to compare the joint TGA group with the control group (p2). To compare all three groups at once (p3), Kruskal–Wallis test was applied. *P*-values greater than or equal to 0.05 were considered to be non-significant (n.s.). Descriptive variables are presented as the mean ± SD and categorical variables as absolute and relative frequencies.

RESULTS

Morphology

The morphological data are presented in Table 1. The aortic root was larger in both TGA groups compared with controls. The ascending aorta was smaller in the spiral group. The cross-sectional area of the left pulmonary artery was smaller in the Lecompte group and the aortic arch was steeper (Fig. 1). The angle of pulmonary to aortic root changed significantly in the spiral group towards control values.

Ventricular and valvular function, aortic elasticity, myocardial perfusion and scar

Ventricular and aortic data are presented in Table 2. No significant differences were found in TGA groups considering myocardial perfusion, or myocardial scar with LGE, ventricular function and aortic

Table 2: Function and perfusion

	Lecompte ($n = 9$)	Spiral ($n = 6$)	*P*-value
LVEF (%)	58 ± 6	60 ± 8	n.s.
LVSV (ml/m^2)	58 ± 9	55 ± 11	n.s.
LVEDV (ml/m^2)	99 ± 15	97 ± 22	n.s.
LVESV (ml/m^2)	41 ± 9	38 ± 17	n.s.
LV mass (g/m^2)	81 ± 46	67 ± 13	n.s.
Aortic RGF (%)	7.9 ± 12.0	4.2 ± 2.5	n.s.
RVEF (%)	56 ± 6	55 ± 8	n.s.
RVSV (ml/m^2)	44 ± 24	50 ± 14	n.s.
RVEDV (ml/m^2)	96 ± 11	91 ± 30	n.s.
RVESV (ml/m^2)	42 ± 7	41 ± 19	n.s.
RV mass (g/m^2)	31 ± 15	29 ± 6	n.s.
Distensibility (10^{-3} mmHg^{-1})			
Ascending aorta at the sinus	3.8 ± 2.5	3.9 ± 1.9	n.s.
Ascending aorta	4.4 ± 1.6	4.0 ± 1.15	n.s.
Descending aorta at isthmus	5.6 ± 2.0	5.2 ± 1.8	n.s.
Descending aorta at diaphragm	7.0 ± 2.8	7.3 ± 2.7	n.s.
PWV (m/s)	4.5 ± 1.2	5.0 ± 0.9	n.s.
Mean arterial pressure (mmHg)	79 ± 11	74 ± 16	n.s.
Semilunar dysfunctions (patients, *n*)	5	1	
Perfusion			
Myocardial perfusion reserve	2.8 ± 1.1	3.0 ± 1.0	n.s.
Rest perfusion (ml/g/min)	1.0 ± 0.4	1.0 ± 0.1	n.s.
Stress perfusion (ml/g/min)	2.6 ± 0.9	2.7 ± 1.1	n.s.
LGE present (*n*)	1	1	

Data presented as mean ± standard deviation.
LVEF: left ventricular ejection fraction; LVSV: left ventricular stroke volume; LVEDV: left ventricular end-diastolic volume; LVESV: left ventricular end-systolic volume; LV: left ventricle; RGF: regurgitation fraction; RVEF: right ventricular ejection fraction; RVSV: right ventricular stroke volume; RVEDV: right ventricular end-diastolic volume; RVESV: right ventricular end-systolic volume; RV: right ventricle; PWV: pulse wave velocity; *n*: number of patients; LGE: late gadolinium enhancement.

elastic characteristics. There were 3 patients in the Lecompte group with mild pulmonary insufficiency (regurgitant fraction 9–20%) and none in the spiral group. Significant pulmonary stenosis was present in 2 patients in the Lecompte group and in 1 of the spiral group (patch plasty of the pulmonary artery). More than trace aortic regurgitation was present in 2 patients of the Lecompte group (i.e. regurgitant fraction 18 and 37%) and in none of the spiral group.

3D time-resolved phase contrast ('4flow')

The phase contrast data on velocity, visual vortex counting and grading of helicity and relative helicity are presented in Table 3 and Figs 2 and 3. The peak blood flow velocity was higher in the aortic arch in the spiral group compared with the Lecompte group. The number of vortices was higher in the Lecompte group. As indicated by the sign of relative helicity results, the flow pattern in control subjects changed from a right-handed to a left-handed helical flow during systole when moving from the ascending aorta towards the aortic arch down the descending aorta supporting previous findings [15]. The spiral group showed the same change in helical flow handedness as the control group. In contrast, the Lecompte group showed a different helical flow pattern: the orientation turned from a left-handed to a right-handed helical flow pattern when moving through the aorta. Owing to the limited number of patients in this study, differences in helical flow patterns—even though visually apparent—were not statistically significant.

The relative helicity magnitude that is used in this study is a dimensionless quantity that indicates the strength of helical flow patterns regardless of the patients' anatomy. In the aorta, relative helicity magnitude was significantly larger in patients who underwent the Lecompte procedure compared with the ones who underwent spiral reconstruction (Fig. 4). Relative helicity in the aorta was not different between patients after spiral reconstruction and controls. In the pulmonary arteries, relative helicity significantly differed among all the three groups and was found significantly larger in the Lecompte group compared with the spiral group (Table 3, Fig. 2).

DISCUSSION

The novel finding in this study is that adult TGA patients 20 years after neonatal spiral anastomoses presented with a more physiological blood flow profiles in their great arteries compared with patients who underwent a Lecompte procedure (Figs 2 and 3). Interestingly, in both groups, the neopulmonary root has rotated leftwards towards the normal anatomical position, significantly more in the spiral group (Supplementary Fig. S2).

Assessment of cardiovascular function

The results of this study suggest that the surgical technique did not have any major influence on aortic bioelasticity, ventricular systolic and diastolic functions, myocardial perfusion and myocardial scar. However, the comparison between the TGA patients and control volunteers confirmed impaired myocardial perfusion [16] and aortic elastic properties, as previously reported by our group (Table 2) [9].

Patients who underwent Lecompte procedure showed a reduced blood flow to their left lungs mainly due to a significantly smaller cross-sectional LPA area that is caused by the rightward position of the pulmonary root, and a pulmonary artery riding on the ascending aorta. Severe pulmonary artery stenosis after Lecompte procedure has also been described in other previous studies [10, 17]. Consistent with this previous finding, we found accelerated blood flow velocities in both pulmonary artery branches (Table 3, Fig. 3) but to a lesser degree compared with the one reported previously [10, 17]. Among the patients who received spiral anastomoses, 1 patient was found to suffer from mild pulmonary stenosis with a maximal gradient of 20 mmHg. This patient had received a pericardial patch elongation for pulmonary artery anastomosis. Refined patch techniques, surgical tailoring of the proximal pulmonary artery or extended mobilization of the peripheral pulmonary arteries may possibly ameliorate this problem and may be favourable to prevent potential left coronary artery compression. It would be interesting to evaluate if the evolution of surgical techniques over the last decades influenced our findings. Mild pulmonary valve insufficiency was identified in 3 patients in the Lecompte group and none in the spiral group, indicating that the leftward rotation of the neopulmonary root may not influence valve function.

Distensibility of the ascending aorta was decreased in both patient groups compared with the controls confirming previous

Table 3: Phase contrast

	Lecompte (n = 9)	Spiral (n = 6)	Control (n = 5)	p1	p2	p3
Vmax (m/s)						
Aortic root	1.34 ± 0.26	1.47 ± 0.12	1.27 ± 0.21	n.s.	n.s.	n.s.
Ascending aorta	1.12 ± 0.26	1.12 ± 0.28	1.26 ± 0.07	n.s.	n.s.	n.s.
Aortic arch	1.21 ± 0.13	1.49 ± 0.08	1.14 ± 0.23	0.019	n.s.	n.s.
Aortic isthmus	1.43 ± 0.14	1.49 ± 0.17	1.33 ± 0.14	n.s.	n.s.	n.s.
Descending aorta	1.70 ± 0.21	1.75 ± 0.30	1.60 ± 0.25	n.s.	n.s.	n.s.
Main pulmonary artery	1.64 ± 0.55	1.56 ± 0.23	1.13 ± 0,21	n.s.	n.s.	n.s.
Right pulmonary artery	1.73 ± 0.30	1.69 ± 0.30	1.18 ± 0.47	n.s.	n.s.	n.s.
Left pulmonary artery	1.66 ± 0.42	1.53 ± 0.15	1.30 ± 0.34	n.s.	n.s.	n.s.
Presence of vortices (n)						
Aorta	4 (44.4%)	0 (0.0%)	–	–	–	–
Pulmonary arteries	2 (22.2%)	2 (33.3%)	–	n.s.	–	–
Relative helicity						
Ascending aorta	−0.056	0.021	0.051			
Aortic arch	0.058	0.042	0.091			
Descending aorta	0.026	−0.017	−0.010			
Relative helicity (mag.)						
Aorta	0.089 ± 0.072	0.036 ± 0.025	0.073 ± 0.049	0.009	n.s.	n.s.
Pulmonary arteries	0.129 ± 0.074	0.085 ± 0.081	0.048 ± 0.055	n.s.	0.003	0.002
Helix severity (visual grading)						
Grading 0	0	4	0			
Grading 1	2	2	0			
Grading 2	7	0	0			

Phase contrast data are presented as mean ± SD. The maximum velocity V_{max} was measured using 2D phase contrast, whereas the other quantities (vortex count, relative helicity, wall shear stress) were measured and determined using 4D phase contrast (4D-flow). *P*-values refer to a comparison of groups: Lecompte and spiral (p1), controls and TGA (p2) and all groups (p3).

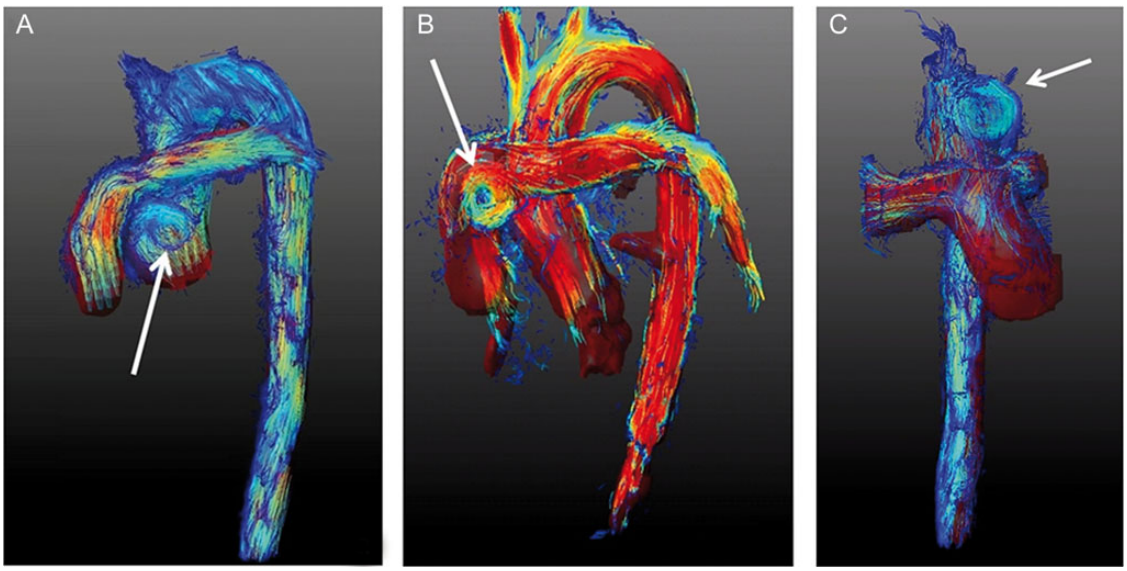

Figure 2: Pathlines in lateral (**A** + **B**) and anterior–posterior view (**C**) two decades after primary ASO with Lecompte, exemplifying vortex formation (arrows) in the great arteries (A: aorta ascending; B: pulmonary artery; C: aorta). The images display the typical steep angle of the aortic arch and the pulmonary bifurcation in front of the ascending aorta. (Full movie available for electronic download.) ASO: arterial switch operation.

reports [9]. Besides a possible genetic background [18], surgical transection, or manipulation of the vasa vasorum [19], or even denervation [20] may impact distensibility. This denervation may also reduce the myocardial perfusion reserve according to our cohort (Table 2) [16]. We found a non-symptomatic coronary stenosis in 1 TGA patient after the spiral technique without regional perfusion deficit. Retrospective review of the surgery report did not indicate any particular anatomical variation.

Surgical considerations from 4D flow magnetic resonance analysis

The Lecompte technique is currently the standard technique [4] but it has been questioned in several independent publications because of its adverse sequelae in some patients in long term [11, 12]. The spiral technique for retransposing the great arteries preserves the physiological Romanesque shape of the aorta in

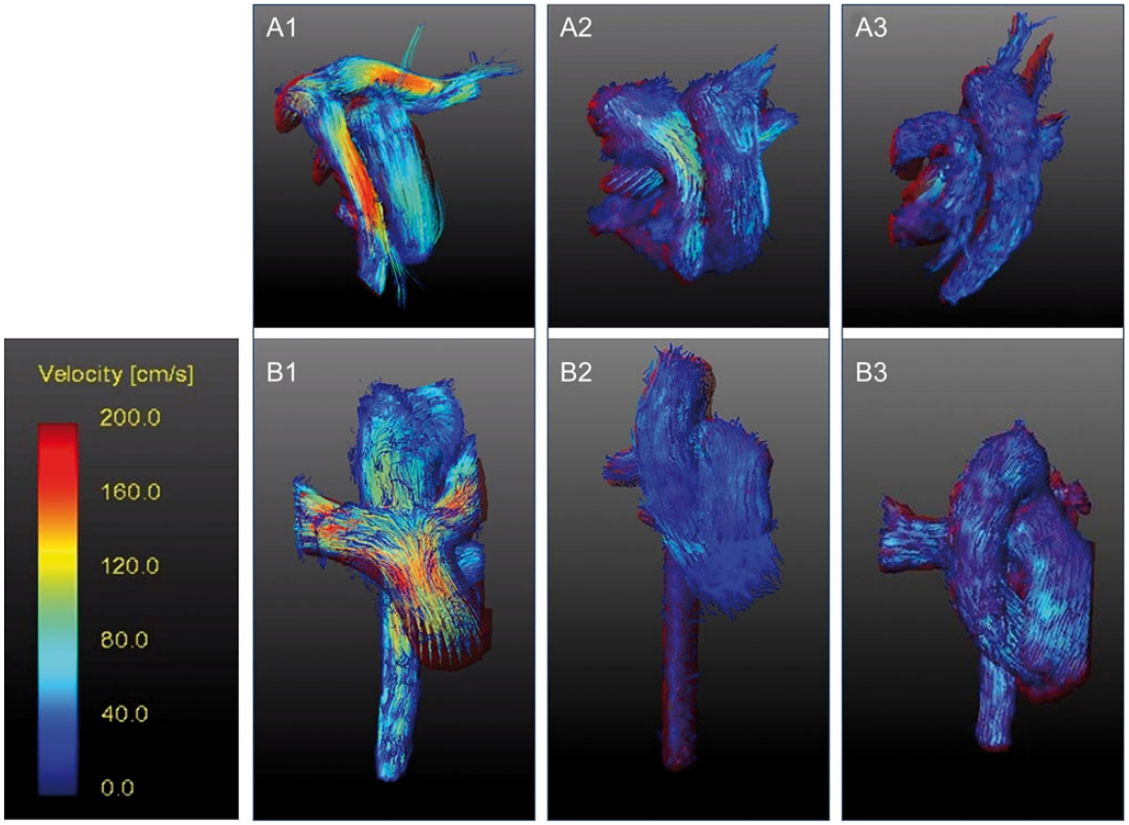

Figure 3: Colour-coded flow velocities in the great arteries displayed from different perspectives (superior view: 1a–3a; anterior view: 1b–3b). Pathlines were reconstructed from 4D flow data for patients after ASO with Lecompte (left), spiral anastomosis (middle) and a healthy volunteer (right). ASO: arterial switch operation.

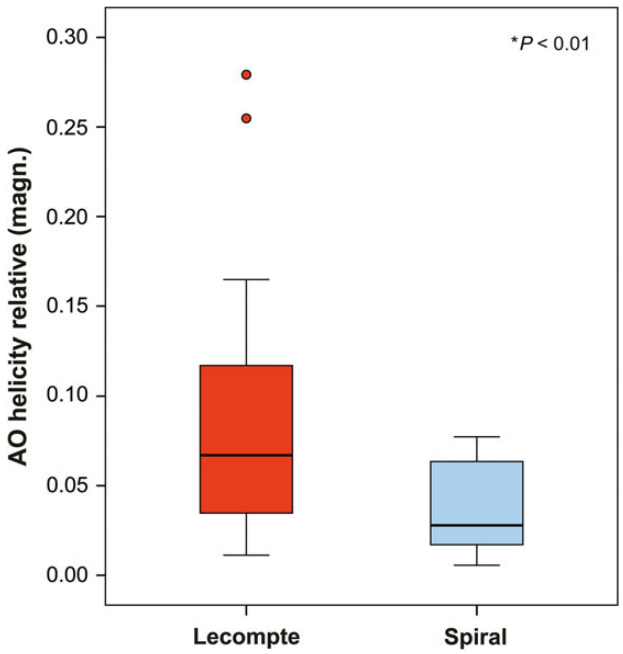

Figure 4: Boxplot illustrating the relative helicity difference of the thoracic aorta in TGA patients after Lecompte or spiral technique. The graph illustrates the higher standard deviation and mean value of helical flow within the thoracic aorta (*Mann–Whitney *U*-test). TGA: transposition of the great arteries.

contrast to the Lecompte technique that resembles a Gothic-shaped arch (Figs 1 and 2). Advanced MRI methods identified a larger number of vortical flow features, more commonly found in the aortic sinus and the main pulmonary artery trunk (Fig. 2A and B) with an increased aortic helical flow (Fig. 2C) in patients who underwent Lecompte technique. The clinical implication of this observation remains speculative.

Kilner *et al.* [21] discussed the favourable effects of the normal looped aortic curvature and the resulting flow characteristics on avoidance of atherogenicity and maintaining 'physically active lifestyle'. They concluded that spatial configurations should be reinstated if technically possible supporting the importance of the present study.

Stronger and more extended helical flow patterns could also be due to the steeper angle of the aortic arch in Lecompte patients, which may have a negative impact on the development of aortic regurgitation as well as systemic hypertension (Supplementary Fig. S2, Table 1) [11, 22]. In the present study, we did not find aortic regurgitation above the trivial levels in the spiral group whereas we found 2 patients with mild (regurgitant fraction 8%) and moderate (regurgitant fraction 37%) insufficiency, respectively, in the Lecompte group. Compared with the age-matched control subjects, our data show that the cross-sectional area of the sinus and the ascending aorta are significantly increased in Lecompte patients (Table 1). However, we found no difference between the spiral and Lecompte groups. Lalezari *et al.* [18] demonstrated that the neoaortic root has some histomorphological deficiencies in collagen content and myocardial support that may explain the neoaortic root dilatation and consequently the aortic regurgitation after ASO. The patients in our cohort showed overall larger aortic root dimensions compared with controls. The riding of the pulmonary artery over the ascending aorta after Lecompte procedure frequently results in flow acceleration or

stenosis of the pulmonary artery and its branches that may lead to a reoperation and/or right ventricular dysfunction [6, 9, 23]; and the dynamic characteristic of this stenosis was shown by Gutberlet *et al.* [24]. Taken together, our 4D flow measurements yielded more physiological blood flow profiles in patients who underwent spiral anastomoses. Whether these findings assume more clinical relevance later in life remains to be evaluated.

Spatial relationship of the great arteries

The negative angle between the aortic and pulmonary root prior to the correction changed in both groups but more significantly in the spiral technique with neopulmonary root being rotated to the left (Table 1), an arrangement that is also observed in the control subjects. Whether this rotation presents some kind of functional plasticity in the outflow tracts after birth remains speculative. It is well known that the cardiac tissue of an infant has not yet finally differentiated bearing the potential for post-surgical remodelling [25]. Unfortunately, sequential MR images during the growth period for these patients are not available to better study the time course of this phenomenon. Whether environmental factors such as mechano-transduction due to tension on the pulmonary artery after ASO contribute to the rotation of the pulmonary root towards a more normal spatial portion is unknown.

Limitations

The number of the patients enrolled in this study is small and patients are partially selected, limiting the statistical evidence. Owing to the overwhelming prevalence of the Lecompte technique, it may in fact be very difficult to perform a larger retrospective comparison study. Furthermore, the quantification of velocity, which is a novel imaging method, needs more investigation on specificity and sensitivity in a larger number of patients. Nevertheless, we think that the results shed some light on the long-term functional outcomes of the two techniques.

CONCLUSIONS

In this study, 20 years after primary correction of TGA, a more physiological blood flow pattern was observed using 4D Flow MRI in patients who underwent spiral anastomoses versus Lecompte technique. This may be due to the closer to normal anatomical position of the great arteries, aortic arch angle, ascending aortic and left pulmonary artery cross-sectional area after spiral anastomoses, when compared with the Lecompte technique. Ventricular function and aortic bioelastic properties were found similar in both groups. Although not significant, there were lesser semilunar valve dysfunctions after spiral anastomosis. The differences between both techniques may find more clinical relevance in the next decades and provoke rethinking of the optimal ASO technique in selected patients.

SUPPLEMENTARY MATERIAL

Supplementary Material is available at *ICVTS* online.

ACKNOWLEDGEMENTS

The authors also thank Traudel Hansen (CMR technologist) for her assistance in patient management.

Funding

This research was also made possible in part through a career development grant from Fondation Leducq to Arash Kheradvar and a postdoctoral fellowship (14POST20530013) from the American Heart Association to Ahmad Falahatpisheh.

Conflict of interest: none declared.

REFERENCES

[1] Liebman J, Cullum L, Belloc NB. Natural history of transposition of the great arteries. Anatomy and birth and death characteristics. Circulation 1969;40:237–62.
[2] Jatene AD, Fontes VF, Paulista PP, de Souza LC, Neger F, Galantier M *et al.* Successful anatomic correction of transposition of the great vessels. A preliminary report. Arq Bras Cardiol 1975;28:461–4.
[3] Lecompte Y, Zannini L, Hazan E, Jarreau MM, Bex JP, Tu TV *et al.* Anatomic correction of transposition of the great arteries. J Thorac Cardiovasc Surg 1981;82:629–31.
[4] Lacour-Gayet F, Anderson RH. A uniform surgical technique for transfer of both simple and complex patterns of the coronary arteries during the arterial switch procedure. Cardiol Young 2005;15(Suppl 1): 93–101.
[5] Pretre R, Tamisier D, Bonhoeffer P, Mauriat P, Pouard P, Sidi D *et al.* Results of the arterial switch operation in neonates with transposed great arteries. Lancet 2001;357:1826–30.
[6] De Praetere H, Vandesande J, Rega F, Daenen W, Marc G, Eyskens B *et al.* 20 years of arterial switch operation for simple TGA. Acta Chir Belg 2014; 114:92–8.
[7] Co-Vu JG, Ginde S, Bartz PJ, Frommelt PC, Tweddell JS, Earing MG. Long-term outcomes of the neoaorta after arterial switch operation for transposition of the great arteries. Ann Thorac Surg 2013;95:1654–9.
[8] Grotenhuis HB, Kroft LJ, van Elderen SG, Westenberg JJ, Doornbos J, Hazekamp MG *et al.* Right ventricular hypertrophy and diastolic dysfunction in arterial switch patients without pulmonary artery stenosis. Heart 2007;93:1604–8.
[9] Voges I, Jerosch-Herold M, Hedderich J, Hart C, Petko C, Scheewe J *et al.* Implications of early aortic stiffening in patients with transposition of the great arteries after arterial switch operation. Circ Cardiovasc Imaging 2013;6:245–53.
[10] Losay J, Touchot A, Capderou A, Piot JD, Belli E, Planche C *et al.* Aortic valve regurgitation after arterial switch operation for transposition of the great arteries: incidence, risk factors, and outcome. J Am Coll Cardiol 2006;47:2057–62.
[11] Agnoletti G, Ou P, Celermajer DS, Boudjemline Y, Marini D, Bonnet D *et al.* Acute angulation of the aortic arch predisposes a patient to ascending aortic dilatation and aortic regurgitation late after the arterial switch operation for transposition of the great arteries. J Thorac Cardiovasc Surg 2008;135:568–72.
[12] Chiu IS, Hung CR. Restoration of transposed great arteries with or without subpulmonary obstruction to nature. In: Nazari S (ed). *Front Lines of Thoracic Surgery*. Rijeka: InTech. 2012.
[13] Jerosch-Herold M. Quantification of myocardial perfusion by cardiovascular magnetic resonance. J Cardiovasc Magn Reson 2010;12:57.
[14] Voges I, Jerosch-Herold M, Hedderich J, Westphal C, Hart C, Helle M *et al.* Maladaptive aortic properties in children after palliation of hypoplastic left heart syndrome assessed by cardiovascular magnetic resonance imaging. Circulation 2010;122:1068–76.
[15] Kilner PJ, Yang GZ, Mohiaddin RH, Firmin DN, Longmore DB. Helical and retrograde secondary flow patterns in the aortic arch studied by three-directional magnetic resonance velocity mapping. Circulation 1993;88: 2235–47.

[16] Hauser M, Bengel FM, Kuhn A, Sauer U, Zylla S, Braun SL *et al*. Myocardial blood flow and flow reserve after coronary reimplantation in patients after arterial switch and ross operation. Circulation 2001;103:1875–80.
[17] Popov AF, Tirilomis T, Giesler M, Oguz Coskun K, Hinz J, Hanekop GG *et al*. Midterm results after arterial switch operation for transposition of the great arteries: a single centre experience. J Cardiothorac Surg 2012;7:83.
[18] Lalezari S, Hazekamp MG, Bartelings MM, Schoof PH, Gittenberger-De Groot AC. Pulmonary artery remodeling in transposition of the great arteries: relevance for neoaortic root dilatation. J Thorac Cardiovasc Surg 2003; 126:1053–60.
[19] Parke WW. The vasa vasorum of the ascending aorta and pulmonary trunk and their coronary-extracardiac relationships. Am Heart J 1970;80:802–10.
[20] Stefanadis CI, Karayannacos PE, Boudoulas HK, Stratos CG, Vlachopoulos CV, Dontas IA *et al*. Medial necrosis and acute alterations in aortic distensibility following removal of the vasa vasorum of canine ascending aorta. Cardiovasc Res 1993;27:951–6.
[21] Kilner PJ, Yang GZ, Wilkes AJ, Mohiaddin RH, Firmin DN, Yacoub MH. Asymmetric redirection of flow through the heart. Nature 2000;404: 759–61.
[22] Ladouceur M, Boutouyrie P, Boudjemline Y, Khettab H, Redheuil A, Legendre A *et al*. Unknown complication of arterial switch operation: resistant hypertension induced by a strong aortic arch angulation. Circulation 2013;128:e466–8.
[23] Klitsie LM, Roest AA, Kuipers IM, Hazekamp MG, Blom NA, Ten Harkel AD. Left and right ventricular performance after arterial switch operation. J Thorac Cardiovasc Surg 2014;147:1561–7.
[24] Gutberlet M, Hoffmann J, Kunzel E, Fleischer A, Sarikouch S, Beerbaum P *et al*. Preoperative and postoperative imaging in patients with transposition of the great arteries. Radiologe 2011;51:15–22.
[25] Martin-Puig S, Fuster V, Torres M. Heart repair: from natural mechanisms of cardiomyocyte production to the design of new cardiac therapies. Ann N Y Acad Sci 2012;1254:71–81.